JACS
JOURNAL OF THE AMERICAN CHEMICAL SOCIETY

ARTICLE

pubs.acs.org/JACS

Three-State Trajectory Surface Hopping Studies of the Photodissociation Dynamics of Formaldehyde on ab Initio Potential Energy Surfaces

Bina Fu, Benjamin C. Shepler,[†] and Joel M. Bowman*

Department of Chemistry and Cherry L. Emerson Center for Scientific Computation, Emory University, Atlanta, Georgia 30322, United States

Supporting Information

ABSTRACT: Full-dimensional, three-state, surface hopping calculations of the photodissociation dynamics of formaldehyde are reported on ab initio potential energy surfaces (PESs) for electronic states S_1, T_1, and S_0. This is the first such study initiated on S_1 with ab initio-calculated spin−orbit couplings among the three states. We employ previous PESs for S_0 and T_1, and a new PES for S_1, which we describe here, as well as new spin−orbit couplings. The time-dependent electronic state populations and the branching ratio of radical products produced from S_0 and T_1 states and that of total radical products and molecular products at three total energies are calculated. Details of the surface hopping dynamics are described, and a novel pathway for isomerization on T_1 via S_0 is reported. Final translational energy distributions of H + HCO products from S_0 and T_1 are also reported as well as the translational energy distribution and final rovibrational distributions of H_2 products from the molecular channel. The present results are compared to previous trajectory calculations initiated from the global minimum of S_0. The roaming pathway leading to low rotational distribution of CO and high vibrational population of H_2 is observed in the present calculations.

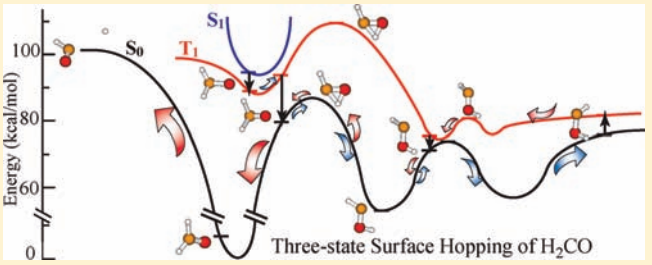

INTRODUCTION

As the prototype for the fundamental understanding of photochemistry, the photodissociation dynamics of formaldehyde have been intensively studied both experimentally[1−17] and theoretically[18−36] for several decades. The interest in H_2CO is further enhanced due to its role in atmospheric, interstellar, and combustion chemistry.

The unimolecular dissociation is initiated by photoexcitation of ground-state $H_2CO(S_0)$ to the first electronically excited singlet state, S_1, followed by internal conversion to S_0 and/or intersystem crossing to the first triplet state, T_1, which can also intersystem cross to S_0. There is a potential barrier of 87 kcal/mol relative to the S_0 global minimum to the formation of molecular products H_2 + CO on S_0 and no potential barrier to the formation of radical products H + HCO, but these have a dissociation energy of 94 kcal/mol. The molecular products exclusively come from S_0; however, the radical products can be produced from both S_0 and T_1. There is also a potential barrier of 99 kcal/mol, relative to the S_0 minimum, to produce radical products on T_1. This is 5 kcal/mol above the dissociation energy on S_0. Thus, depending on the excitation energy, the reaction products can be solely H_2 + CO, or if sufficiently high, the radical channel may compete with the molecular one. At excitation energies that exceed the barrier on the T_1 surface, the radical channel on T_1 also contributes to the radical products.

Moore and co-workers have done pioneering experiments at photolysis energies where the molecular products H_2 + CO are exclusively produced.[1−5] The details of the experimental work as well as the photodissociation mechanism were reviewed previously by Moore and Weisshaar[1] and Green et al.[4] Theoretical work, mostly quasiclassical trajectory (QCT) calculations, has also focused on the reaction dynamics for the molecular channel on S_0,[18−23] and until 2004, the QCT calculations were initiated at the well-known molecular product's transition state (TS).[19−23] These calculations showed that the CO rotational distribution was Gaussian-like with a peak at j_{CO} around 40, which was in agreement with experiment. However, in 1993, van Zee et al.[5] discovered that, near the threshold of the H + HCO channel, the CO rotational distributions exhibited a curious shoulder at low values of j_{CO}. The source of this feature was elucidated in 2004 by a joint experimental and theoretical investigation.[24] In that work, a second pathway was reported that yields rotationally cold CO and vibrationally hot H_2. This second pathway was denoted the "roaming" H atom pathway because it bypasses the molecular TS and is characterized by incipient formation of the radicals, which, however, do not have enough energy to dissociate, but instead orbit each other followed by H atom self-abstraction to form H_2 + CO.[25−28] The QCT calculations performed in that study were done on a global S_0 potential energy surface,[29] which contains both the molecular and radical channels. The trajectories were

Received: February 18, 2011
Published: April 28, 2011

dx.doi.org/10.1021/ja201559r | J. Am. Chem. Soc. 2011, 133, 7957–7968

initiated from the H_2CO minimum, not from the molecular TS, as was done in all previous calculations.[19−23]

By contrast to studies of the molecular products, only limited experimental and theoretical studies have focused on the radical products H + HCO.[8−17] These (ground electronic state) products can be formed on both S_0 and T_1, and the HCO rotational distributions and relative translational energy distributions display signatures of these two different electronic pathways. Bowman and co-workers performed QCT calculations[24−28] using a global potential energy surface (PES) for S_0[29] and a semiglobal T_1 PES.[27] The S_0 calculations were initiated from the global minimum, as already noted, while those on T_1 were initiated from the relevant T_1 saddle point, and no coupling of the two surfaces was considered. The results of these calculations were in good agreement with experiment on the signatures of the HCO rovibrational energy distributions.[14] However, neither experiment nor theory has previously determined the fraction of HCO originating from T_1 or S_0.

More recently, theoretical work has begun to consider the coupling among S_1, T_1, and S_0 electronic states. A high-energy conical intersection between S_1 and S_0 was reported by Simonsen et al.[30] Further investigations of this intersection were reported shortly thereafter by Araujo et al.[31] Subsequently, Shepler et al.[32] reported the first QCT studies aimed at considering surface intersections. They argued that the high energy of the conical intersection between S_1 and S_0 probably precludes that intersection from being very relevant to existing experiments, including the recent ones that uncovered the roaming pathway to molecular products, and instead focused on lower energy T_1/S_0 intersections. Specifically, they initiated QCT calculations at the T_1/S_0 minimum-energy-crossing configurations in the hydroxycarbene region of configuration space (which were newly reported in that paper). They used a new S_0 PES that contained additional electronic energies in the HCOH region. That PES is used in the present study. The product state distributions of H_2 + CO, including the roaming pathway, were in good agreement with earlier ones that were initiated at the S_0 global minimum. Subsequent to that study, Zhang et al.[33] presented a more extensive study of T_1/S_0 crossings as well as a global PES for the T_1 state. They reported a large barrier on T_1 to isomerization from the T_1 global minimum, which has a nonplanar distorted $H_2CO(S_0)$ structure, to the hydroxcarbene isomers where the minimum T_1/S_0 intersections occur. Therefore, they concluded that those intersections are not relevant to photodissociation experiments. Instead, they concluded that a somewhat higher energy T_1/S_0 intersection in the H_2CO region (with a "strong" spin−orbit coupling of 52 cm^{-1}) is the likely "route" from T_1 to S_0. No dynamics calculations were reported in that study nor in a subsequent one which revisited the S_1/S_0 intersection.[34]

Limited, approximate quantum wavepacket calculations involving T_1/S_0 and S_1/S_0 crossings have recently been reported by Robb and co-workers[35,36] using the direct-dynamics, CASSCF, variational multiconfiguration Gaussian (DD-vMCG) wavepacket method, implemented in a development version of the Heidelberg MCTDH package,[37] coupled to the Gaussian quantum chemistry program.[38] These studies have in common a proposed mechanism for the formation of molecular products H_2 + CO that occurs in the incipient H−HCO region without visiting the region of the H_2CO global minimum. The S_1/S_0 intersection, as already noted, is not likely to play a significant role for the energy range considered experimentally and theoretically to date, so we do not comment further on it. The wavepacket calculations investigating T_1/S_0 dynamics could not be run for long times, owing to the large computational cost, even with the highly approximate CASSCF method, so only "prompt" dynamical events could be studied. These included dissociation to H + HCO and also some evidence of formation of molecular products, depending on the initial conditions, which do not visit the deep portion of the H_2CO global minimum. Final rovibrational analysis of the products was not reported in these exploratory and stimulating calculations.

Clearly then, as we and others have pointed out, full three-state dynamics calculations are needed to (a) validate or invalidate the predictions based on one-state S_0 dynamics, (b) assess the possible importance of recently proposed excited-state pathways to molecular products, and (c) perhaps uncover totally novel reaction pathways. We have done such calculations and report the results here. To do this, with as few assumptions as possible, we use classical trajectory surface hopping, specifically Tully's fewest-switches surface hopping algorithm,[39,40] with the additional time uncertainty algorithm of Jasper and Truhlar.[41]

Initially we investigated a direct-dynamics approach, with the approximate CASSF method, used by Robb and co-workers, but quickly concluded, on the basis of experience with the simpler system OH* + H_2 that this was computationally impractical.[42] Instead, we use full-dimensional PESs, obtained from fitting high-level ab initio calculations. As noted already, such PESs exist for S_0 and T_1, and here we report a new PES for S_1. We also report spin−orbit coupling calculations between S_1 and T_1 and T_1 and S_0. These PESs and couplings are used in extensive, long-time surface hopping calculations in a diabatic representation, using the "ANT2009" code of Truhlar and co-workers.[45] A total of roughly 20 000 trajectories are initiated on S_1 with coordinates and momenta sampled from a Wigner distribution describing the zero-point phase space of $H_2CO(S_0)$. Three total energies are considered, 99.1, 108.6, and 121.1 kcal/mol, relative to the $H_2CO(S_0)$ global minimum.

The paper is organized as follows. First, we present the details of the new S_1 PES and a brief review of the published PESs for T_1 and S_0. We discuss their intersections and spin−orbit couplings. After that, details of the surface hopping methodology and initial conditions are given. The results of surface hopping studies at three total energies on the coupled PESs are given next. These results include time evolution of the nuclear motion on the three electronic states, branching ratios of molecular products and radical products and also those of radical products coming from S_0 and T_1, and new dynamical mechanisms. In addition, the final translational energy distributions of H + HCO, as well as the final translational energy and rovibrational distributions of H_2 + CO, are calculated. A summary and conclusions are given in the final section of the paper.

■ POTENTIAL ENERGY SURFACES AND SPIN−ORBIT COUPLINGS

A global S_0 PES for formaldehyde was reported previously[29] on the basis of CCSD(T)/aug-cc-pVTZ and MRCI/aug-cc-pVTZ calculations and used in a number of dynamics investigations of the H_2CO system.[24,27,46,47] Recently, to better describe the regions around the minimum energy crossings of the T_1 and S_0 surfaces, 1505 more CCSD(T)/aug-cc-pVTZ energies were added to fit a new and improved PES.[32] The interested reader is referred to refs 29 and 32 for the details of the S_0 PES. On the whole, seen from the good agreement between the experimental

and dynamics results on this PES, the current PES we employed is the most accurate global S_0 PES of H_2CO available.

The global T_1 PES used here is due to Zhang et al.[33] That PES is a fit to MRCI(Q)/aug-cc-pVTZ energies by a least-squares method employing a many-body expansion in which each term is a function of the internuclear distances that is invariant under permutations of like atoms.[48] The PES covers the formaldehyde and the HCOH regions as well as the H + HCO dissociation channel. The high quality of the T_1 PES was demonstrated by the low root-mean-square fitting error and close agreements between the critical points from ab initio calculations and from the fitted PES.

The open-shell singlet character of the S_1 PES requires a multireference treatment to obtain a correct description. Therefore, the internally contracted multireference configuration interaction (singles and doubles) method with the multireference analogue of the Davidson correction (MRCI(Q)) was selected. The orbitals for the MRCI(Q) calculations were taken from state-averaged complete-active-space self-consistent field (SA-CASSCF) calculations. The active space used in both the CASSCF and MRCI(Q) calculations was 10 electrons in 8 orbitals and was chosen because it gave a consistent description of the wave function across the large regions of the PES of interest. The S_0, T_1, and S_1 states were all included with equal weights in the SA-CASSCF calculations, while the S_0 and S_1 states were included in the MRCI(Q) calculations. The cc-pVDZ, aug-cc-PVDZ, cc-pVTZ, and aug-cc-pVTZ basis sets were tested in benchmark calculations on a number of stationary points. The cc-pVTZ set was found to be the best compromise between accuracy and efficiency and was used for the computation of the PES. All the ab initio calculations were done by the quantum chemistry program MOLPRO.[49]

In total, 18 424 MRCI(Q)/cc-pVTZ energies were used to fit the S_1 PES. The configuration-space sampling was accomplished by a mixture of grid sampling and random displacement of Cartesian coordinates about stationary points and other points of interest (conical intersections). The PES was fit using a basis of permutationally invariant polynomials following a procedure developed in our group and used recently to fit a large number of global PESs.[48] Specifically, the fit used a basis of permutationally invariant polynomials of Morse-like variables in all internuclear distances [$y_{ij} = \exp(-r_{ij}/\lambda)$, where $\lambda = 2.0$ bohr]. The fit included all basis functions up to sixth order for a total of 530 coefficients. These associated coefficients were obtained by standard linear least-squares fitting to all the data. The weighted rms error of the fitted surface is 1.1 kcal/mol for energies up to 60.0 kcal/mol relative to the global minimum of S_1.

A schematic representation of the S_1 PES is given in Figure 1. Energies, relative to the S_1 minimum, and structures are shown for the present MRCI(Q)/cc-pVTZ optimized stationary points and those from the PES. The minimum of the S_1 state is of nonplanar C_s geometry, and the indicated stationary structure of the C_{2v} symmetry is a saddle-point TS connecting two equivalent C_s minima, with a barrier of 3.6 kcal/mol from the fitted PES with zero-point energy (ZPE) correction, compared to 4.0 kcal/mol from MRCI(Q)/cc-pVTZ calculations. The single minimum on the HCOH side of C_1 symmetry is 26.0 (26.5) kcal/mol, where the value in parentheses is the ab initio value, above the S_1 state minimum. The two corresponding *cis* and *trans* structures are shown to be the TSs connecting the C_1 minimum, with energies of 33.4 (33.7) and 28.8 (29.3) kcal/mol, respectively. The TS for isomerization to HCOH in C_1 symmetry is 53.4 (53.7) kcal/mol, which corresponds to a reverse reaction barrier of 27.4 (27.2) kcal/mol

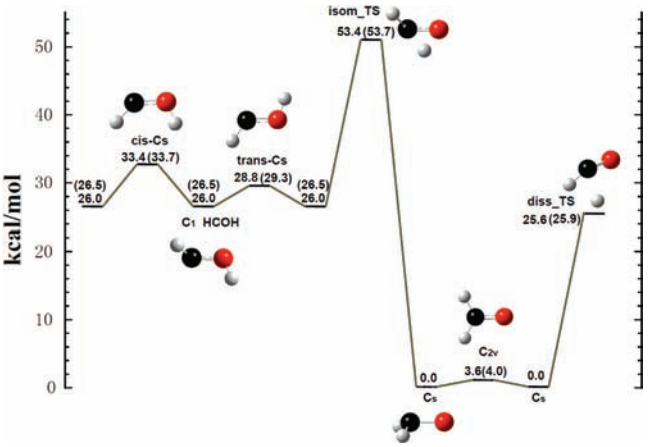

Figure 1. Schematic of the H_2CO S_1 potential energy surface showing stationary points and energies, relative to the S_1 minimum (ZPE-corrected), from the new fitted PES and MRCI(Q)/cc-pVTZ energies (shown in parentheses).

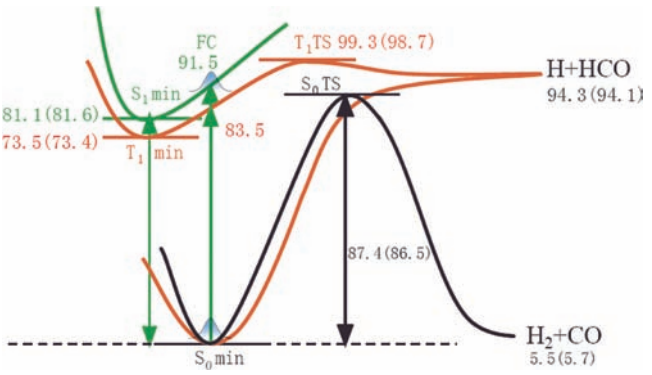

Figure 2. Sketch of the energies (kcal/mol) of the S_0, T_1, and S_1 states of H_2CO in the Franck−Condon region relevant to the present calculations. Energies shown in parentheses are from MRCI(Q)/aug-cc-pVTZ calculations.

relative to HCOH. The TS connecting the C_s minimum and the excited-state dissociation products $HCO(^2\Pi)$ + H (labeled diss_TS) is of C_1 symmetry and energetically lies 25.6 (25.9) kcal/mol above the minimum. From the comparisons we can see the properties obtained from the fitted PES and MRCI(Q)/cc-pVTZ calculations agree very well. We also found these properties calculated by the present cc-pVTZ basis are close to those obtained with the aug-cc-pV5Z basis,[33] with an average difference of 1.2 kcal/mol, which again verifies that the cc-pVTZ basis set was ideal in this study when both accuracy and efficiency were considered.

We note that the three PESs were calculated on the basis of different levels of ab initio theory, so small adjustments to their absolute energies were done. Specifically, the T_1 and S_1 PESs were shifted so that vertical excitation energies from the S_0 global minimum to T_1 and S_1 are in agreement with calculated MRCI(Q)/aug-cc-pVTZ values. The resulting energies, relative to the S_0 global minimum, of these three PESs are summarized graphically in Figure 2. As indicated, the vertical excitation energy from S_0 to T_1 is 83.5 kcal/mol, and that from S_0 to S_1 is 91.5 kcal/mol, so the vertical excitation energy from T_1 to S_1 is 8 kcal/mol. We also see that the energies of the global minimum on T_1 and S_1 PESs are

dx.doi.org/10.1021/ja201559r |J. Am. Chem. Soc. 2011, 133, 7957–7968

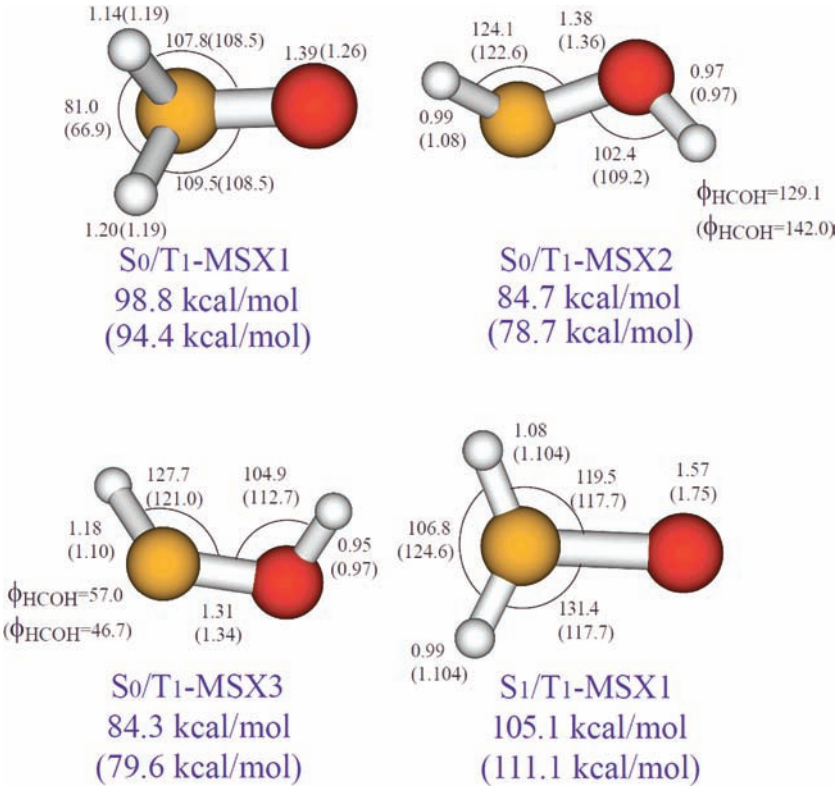

Figure 3. Structures (Å, deg) and energies (kcal/mol) relative to the H_2CO S_0 global minimum of three MSXs indicated located on the PESs, compared to those obtained by Zhang et al.[33] and one (S_1/T_1 MSX1) from Maeda et al.[34] (shown in parentheses).

73.5 and 81.1 kcal/mol relative to that on S_0, which are in good agreement with the MRCI(Q) aug-cc-pVTZ values of 73.4 and 81.6 kcal/mol, respectively. Furthermore, the potential energies of the radical channel on S_0 and T_1 are accurately given as 94.3 kcal/mol, relative to the S_0 minimum, compared to the ab initio results of 94.1 kcal/mol. Also, note that there exists a saddle-point TS state to form the radical products on T_1, though no barrier on S_0 for that channel. As seen, the barrier height on the T_1 PES is 99.3 kcal/mol relative to the S_0 minimum, in accord with the MRCI(Q) result of 98.7 kcal/mol. Also the properties on the S_0 PES are of course not changed compared to the results reported before, with a barrier of 87.4 kcal/mol (86.5 kcal/mol for the MRCI calculation) and a dissociation energy of 5.5 kcal/mol (5.7 kcal/mol) to form H_2 + CO products. A sketch of the ground vibrational state density is also indicated.

Next we consider the energies of various PES intersections and compare them to the recent direct calculations of Zhang et al.,[33] who reported several minimum crossing points on the S_0/T_1 intersection seams (minimum surface crossings, MSXs) on the basis of MRCI(Q)/aug-cc-pVTZ calculations, and Maeda et al.,[34] who reported one S_1/T_1 minimum energy crossing seam using CASPT2/aug-cc-pVDZ calculations. Before those works two of the S_0/T_1 crossings in the hydroxycarbene region of configuration space had been reported by Shepler et al.[32] We also located these MSX structures on our S_0, T_1, and S_1 PESs by constrained geometry optimizations using the Lagrange−Newton method[50] and show the results in Figure 3. The structures and energies relative to the S_0 minimum of the three S_0/T_1 MSXs and one S_1/T_1 MSX are compared to the results obtained previously.[33,34] Among the three S_0/T_1 MSXs, MSX1 has a formaldehyde-like structure, MSX2 a *trans*-HCOH structure, and MSX3 a *cis*-HCOH structure. We can clearly see both the geometries and energies of MSXs located on our PESs are close to the previous ones.[34,35] These have the maximum energy difference of 6 kcal/mol, which is small compared to the energies of the potentials at the crossings. It should also be noted that these crossing geometries and energies are very sensitive to the level of ab initio theory and basis because they often occur when one potential at least is varying rapidly with the nuclear configuration.

We calculated the magnitude of the spin−orbit (SO) couplings between S_1 and T_1 and T_1 and S_0 using MRCI/aug-cc-pVTZ calculations with MOLPRO.[49] As is typically done, e.g., the recent study of spin−orbit coupling in the $O(^3P) + C_2H_4$ reaction by Schatz and co-workers,[51] these are the couplings that are used in diabatic-state surface hopping calculations. These will be described in detail in the following subsection. We note that the triplet−singlet SO coupling matrix is 4 × 4; however, as is typically done, e.g., by Morokuma and co-workers,[33] the norm of the SO matrix is used to describe the coupling between the singlet and triplet surfaces. This leads to a simplified description of the coupling between the triplet and a given singlet surface as a two-state interaction. This simplification is reasonable as the SO coupling in the present case is quite small and only very slightly splits the degeneracy of the spin-free triplet state. (It is also in accord with previous work, for example, that of Schatz and co-workers mentioned above.)

To investigate the magnitude and variation of the SO couplings, consider first the variation of the SO coupling with the increase of one of the CH internuclear distances from the three crossings MSX1, MSX2, and MSX3. These are shown in parts a−c, respectively, of Figure 4. As seen, the SO magnitudes of S_0/T_1 and S_1/T_1 behave quite differently. The SO magnitudes

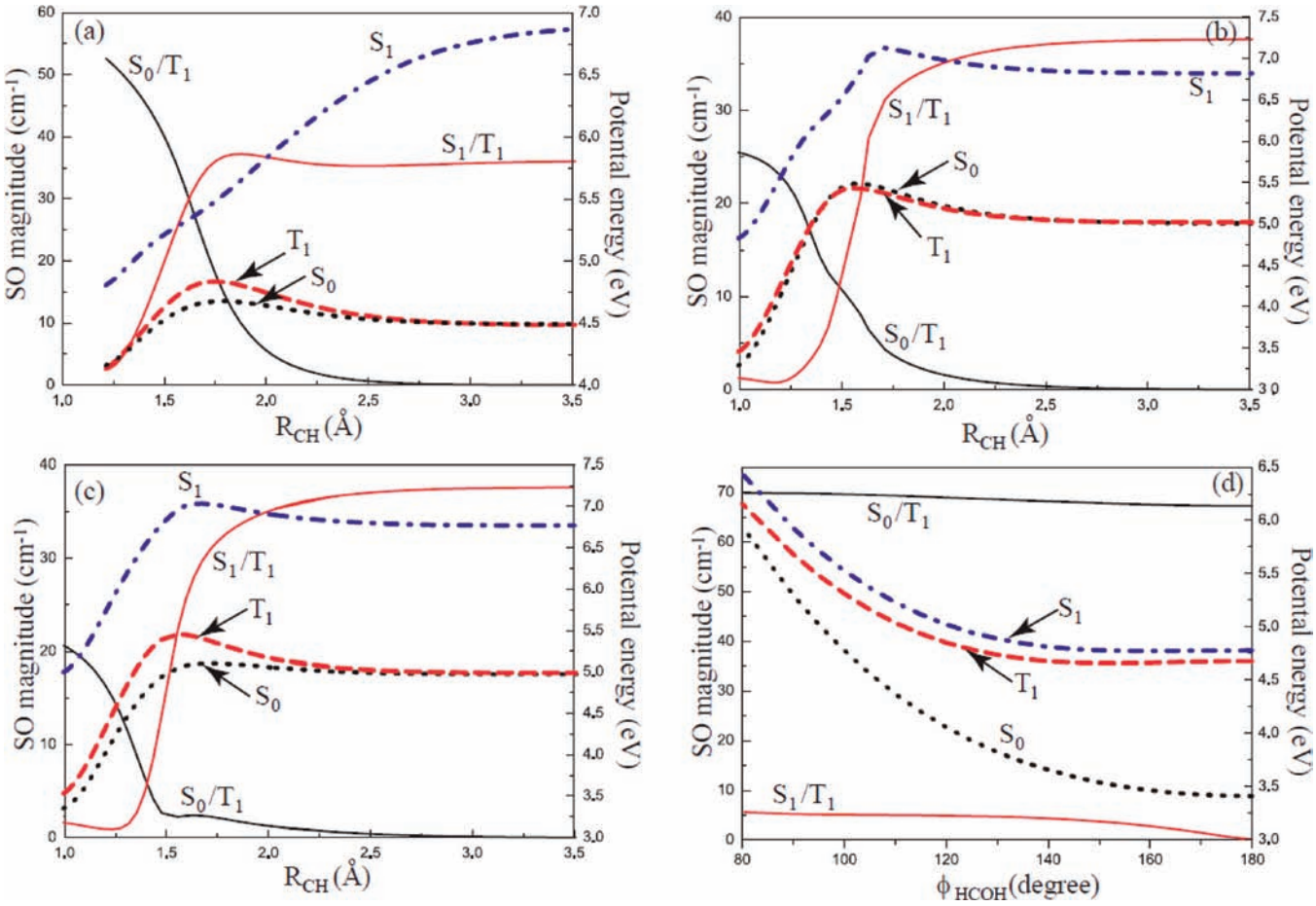

Figure 4. Calculated SO coupling magnitudes (left *y*-axis, cm^{-1}) and potential energies of three states (right *y*-axis, eV) calculated as a function of one of the internuclear distances of CH (R_{CH}) or the dihedral angle ϕ_{HCOH}, with the remaining degrees of freedom fixed, starting at the four MSX structures shown in Figure 3. (a) is for S_0/T_1 MSX1, (b) for S_0/T_1 MSX2, (c) for S_0/T_1 MSX3, and (d) for S_1/T_1 MSX. The solid lines are for the SO magnitudes (black for S_0/T_1, red for S_1/T_1), and the dashed lines are for the potential energies (black for S_0, red for T_1, and blue for S_1).

for S_0/T_1 obtained at the MSXs are larger, and the largest one is that at the MSX1 structure with a value around 60 cm^{-1} shown in Figure 4a. As the configurations move away from the S_0/T_1 seams of crossing structures, the SO magnitudes between S_0 and T_1 decrease monotonically and vanish at the H + HCO asymptote, where the potential energies of S_0 and T_1 are degenerate, while those between S_1 and T_1 increase and become nearly constant with a value of 30 cm^{-1}. It should be emphasized that when the SO magnitude of S_1/T_1 is larger than 5 cm^{-1}, the potential energy of S_1 is above the energies considered here, and thus, the dynamics in that region is of little importance. We also calculated the SO magnitudes away from the S_1/T_1 MSX structure and show the results as a function of the dihedral angle ϕ_{HCOH} in Figure 4d. All other internal coordinates are fixed at the S_1/T_1 MSX. As seen, the SO magnitudes of S_1/T_1 vary from 0 to 5 cm^{-1}, and those of S_0/T_1 remain nearly constant at around 65 cm^{-1}. We note that S_0/T_1 SO couplings at MSX1, MSX2, and MSX3 have been reported recently by Morokuma and coworkers,[33] and the present ones are in very good agreement with those results.

Ideally, we would like to have a global representation of the SO coupling as a function of all internal coordinates; however, that is computationally very expensive and probably not necessary, since, as seen, the SO coupling is nearly a constant in the vicinity of the surface crossings. Thus, we use a simple, but reasonable approach, which is to assume a constant value of 60 cm^{-1} for the SO coupling for S_0/T_1, except in the H + HCO asymptotic region, where the coupling vanishes. We also used a constant value of the SO coupling, 5 cm^{-1}, for S_1/T_1. As discussed in the Results and Discussion, hopping takes place in the vicinity of the surface crossings, but rarely at the crossings, and we did verify that at the actual hopping configurations the SO coupling is very close to the constant values assumed. We also performed limited "diagnostic" calculations with an artificially smaller constant SO coupling for S_0/T_1 of 30 cm^{-1}. The only result that changed significantly was the branching ratio between T_1 and S_1 to form the H + HCO products.

TRAJECTORY SURFACE HOPPING CALCULATIONS

The surface hopping calculations require initial conditions, as usual. For photodissociation studies such as the present ones, the ground vibronic state Wigner distribution is typically used to select the initial conditions on the excited-state potential, here S_1.[52−57] The Wigner distribution function for the vibrational ground state of a one-dimensional harmonic oscillator, *i*, is the product of two Gaussian functions, one describing the *q*-space and the other describing the *p*-space, which can be

dx.doi.org/10.1021/ja201559r |J. Am. Chem. Soc. 2011, 133, 7957–7968

expressed as

$$\Gamma_i(q_i, p_i) = \frac{1}{\pi\hbar} e^{-m_i\omega_i q_i^2/\hbar} e^{-p_i^2/(m_i\omega_i\hbar)} \quad (1)$$

where ω_i is the harmonic frequency.

The zero-point wave function for formaldehyde in the S_0 state is approximated by the separable harmonic normal-mode wave function in six normal modes, with coordinates and momenta denoted collectively as $\{q_i, p_i\}$. Thus, the full-dimensional wave function is simply a product of six uncoupled one-dimensional harmonic wave functions, and the corresponding Wigner distribution function can then be expressed as

$$P_W(q_1, p_1, ..., q_6, p_6) = \prod_{i=1}^{6} \Gamma_i(q_i, p_i) \quad (2)$$

The von Neumann acceptance−rejection method[58] was used to generate thousands of initial values of normal-mode coordinates and momenta, subject to the condition of the known harmonic zero-point energy of H_2CO on S_0.

The photoexcitation from the S_0 state to the S_1 state is assumed to be a Franck−Condon process in which the initial (Wigner) phase-space distribution is promoted vertically and unchanged onto the excited S_1 surface, because the transition moment is taken to be constant. Then a phase point is accepted for a trajectory calculation if it is on the "energy shell" according to a procedure described previously.[59,60] In brief, the phase point is accepted if the energy of the S_1 Hamiltonian at that phase point is within $\pm\varepsilon$ of the given total energy E, which is the sum of the photon energy plus the H_2CO (S_0) zero-point energy. ε was chosen as 0.024 eV (0.55 kcal/mol). This value is comparable to values used in previous QCT calculations.[59,60] In this study, three total energies are selected to simulate the photodissociation of formaldehyde, 82, 91.5, and 105 kcal/mol, corresponding to wavelengths of 348, 312, and 272 nm, respectively. Adding the zero-point energy of $H_2CO(S_0)$ gives final total energies of 99.1, 108.6, and 122.1 kcal/mol.

The lowest total energy of 99.1 kcal/mol is just below the barrier on T_1 to form the radical products. In fact, a very small number of these products are formed because adding an ε value of 0.55 kcal/mol does result in some initial conditions which just exceed the barrier height. Thus, the energies considered span a range where radical products from T_1 are virtually energetically forbidden to very energetically allowed. Most of the results here are for a total energy of 108.6 kcal/mol. We performed roughly 13 000 trajectories at this total energy and roughly 3000 trajectories at each of the higher and lower energies.

The trajectory surface hopping method employed in our calculations of the photodissociation of formaldehyde is a modified version of the well-known Tully fewest-switches trajectory surface hopping algorithm[40] with the extension of the time uncertainty algorithm.[41] The diabatic representation is used for the coupled three states of the H_2CO system, and the potential energy matrix is expressed as

$$\begin{bmatrix} V_{11} & V_{12} & V_{13} \\ V_{21} & V_{22} & V_{23} \\ V_{31} & V_{32} & V_{33} \end{bmatrix} \quad (3)$$

where V_{11}, V_{22}, and V_{33} are the potential energies of S_0, T_1, and S_1, respectively, V_{12} represents the spin−orbit coupling between S_0 and T_1, V_{23} denotes the spin−orbit coupling between S_1 and T_1, discussed in detail already, and V_{13} is 0 as there is no spin−orbit coupling between S_0 and S_1.

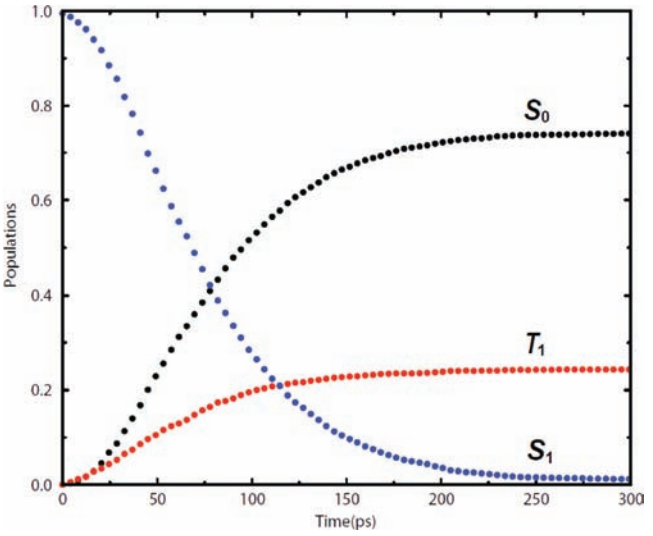

Figure 5. Populations of the electronic states S_1, T_1, and S_0 as a function of time (ps) at a total energy of 108.6 kcal/mol corresponding to a photolysis wavelength of 312 nm.

The hopping probability along a trajectory as a function of time from state i to state j in the diabatic representation is given in refs 40 and 41, and we refer the interested reader there for details. The surface hopping trajectory calculations were performed using the ANT2009 program of Truhlar and co-workers,[45] using the Wigner distribution for the initial conditions. Also, we note that the "stochastic decoherence" option in the code was not used.

RESULTS AND DISCUSSION

First, consider the time dependence of the normalized populations, P_i, of the electronic states S_1, T_1, and S_0. At $t = 0$, $P_{S_1}(t)$ is 1 and all other populations are 0. At any later time t, these populations are determined simply by determining the number of trajectories on each electronic state and dividing by the total number of trajectories. The results for a total energy of 108.6 kcal/mol are shown in Figure 5 at time intervals of 0.2 ps. (The results shown are directly from the data and are not a fit to the data.) As seen, the population of S_1 decays slowly from 1.0, while those of T_1 and S_0 increase, as time increases, as expected. The asymptotic values of the populations are simple to interpret. First, $P_{S_1}(t)$ goes to 0 because no products are formed from this state as all if its population eventually transfers to T_1. The T_1 population can transfer to S_0 but can also decay irreversibly to make the products H + HCO, which are still assigned to T_1 as t goes to infinity. Probability transferred to S_0 eventually leads irreversibly to products H_2 + CO and H + HCO. Thus, the asymptotic ratio of $P_{S_0}(t)$ to $P_{T_1}(t)$ is the ratio of all the products for S_0 to the radical products from T_1.

These populations display apparent, first-order kinetic time dependences. First, note that it takes roughly 100 ps for the population of S_1 to be reduced to 1/e of the initial value. The early time population growth of S_0 and T_1 appears nearly at the same time, and this is due to rapid hopping down to S_0 from T_1 for some trajectories. Second, $P_{T_1}(t)$ is close to its asymptotic value at about 150 ps, indicating that all trajectories on T_1 have led to the H + HCO products at that time. The products on S_0 are produced at

dx.doi.org/10.1021/ja201559r |J. Am. Chem. Soc. 2011, 133, 7957–7968

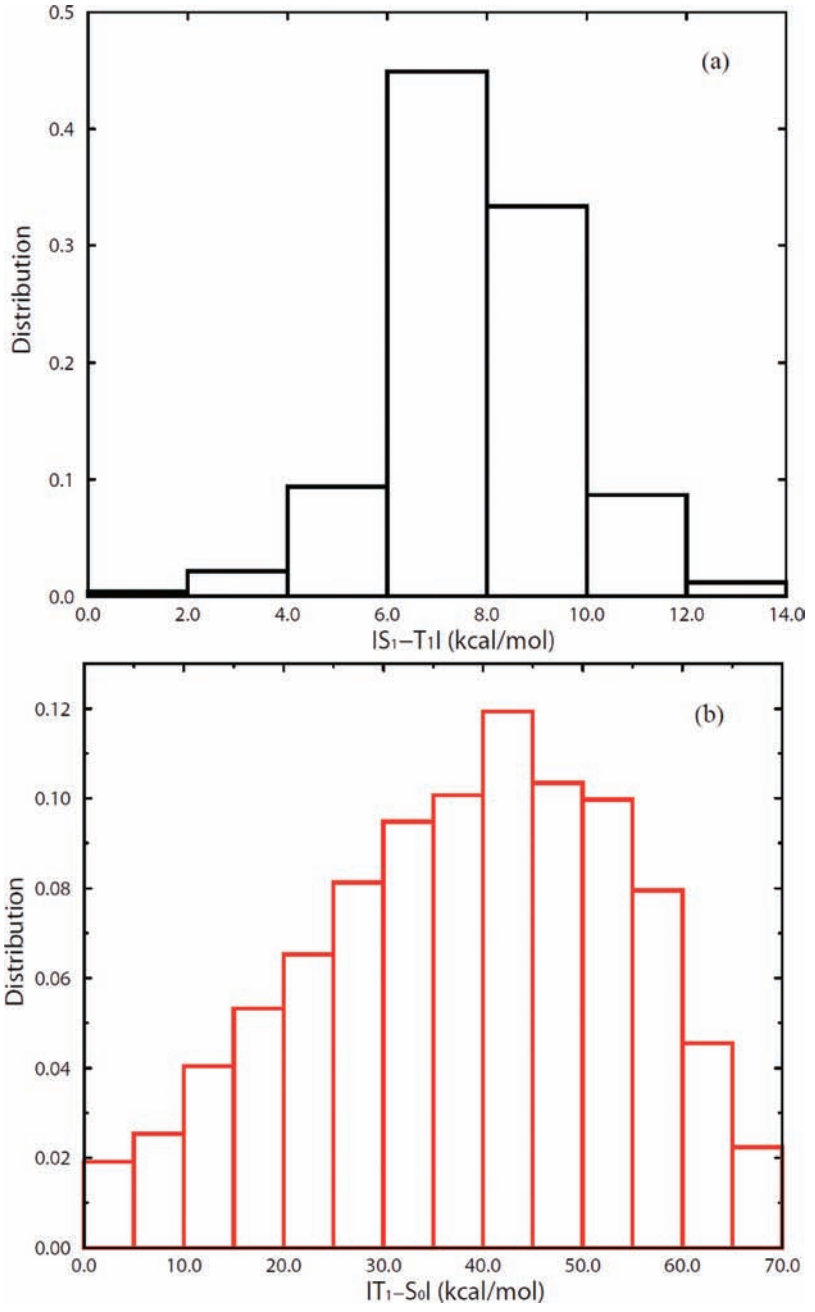

Figure 6. Distributions of energy gaps at the hopping configurations between (a) S_1 and T_1 and (b) T_1 and S_0 at a total energy of 108.6 kcal/mol.

about 200 ps. Very approximately, the population transfers are initially governed by coupling of the three states and then later reflect the dissociation times on the T_1 and S_0 PESs to make products. This is an oversimplification because the three-state coupling vanishes only in regions where the products are nearly formed; however, as shown below, and as already noted, the regions where hops occur is where PESs either intersect or come "close" to each other.

A number of experimental measurements of fluorescence lifetimes of $H_2CO(S_1)$ were reported in the late 1970s and 1980s.[8,61,62] The most recent (1987) paper on the photodissociation of HDCO used such measurements, together with the measured H/D branching ratio in the radical channel to "estimate" an S_1/T_1 crossing rate of 4×10^7 s^{-1} at a total energy "near the top of the T_1 barrier" to dissociation to radical products. This estimate, which was made on the basis of additional dynamical assumptions (see below), would correspond to an S_1 lifetime roughly 100 times longer than the lifetime from the present calculations. It is certainly the case that the time dependences shown here are sensitive functions of the SO couplings and the underlying complex dynamics, which are described classically, on the PESs. It is possible that the assumptions made to determine the above experimental estimate, i.e., a unit quantum yield for dissociation to radical products from T_1 and no production of D atoms from T_1 (only from S_0), are not valid. (In fact, we do not see a unit quantum yield to form radical products from T_1.) This is clearly an issue that is beyond the scope of the current paper, but one that should stimulate future work, both experimental and theoretical, on this aspect of the multistate dynamics.

dx.doi.org/10.1021/ja201559r |J. Am. Chem. Soc. 2011, 133, 7957–7968

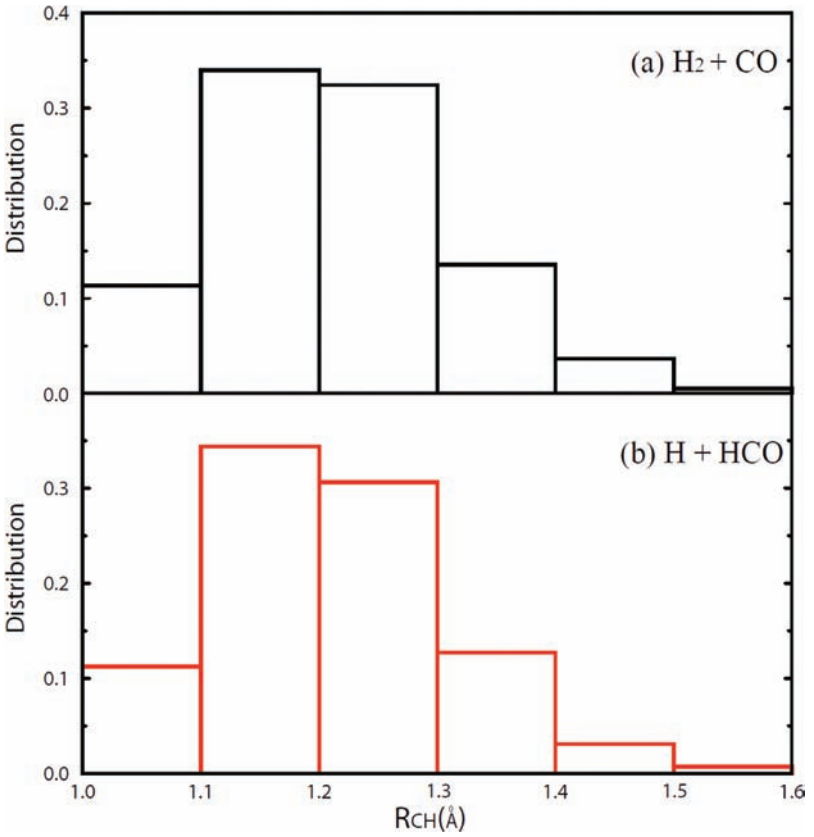

Figure 7. Distributions of the most extended CH bond length at the first hopping configuration from T_1 to S_0 to form (a) $H_2 + CO$ and (b) $H + HCO$ products at a total energy of 108.6 kcal/mol.

It is perhaps also worth noting that propagating trajectories or wavepackets for the hundreds of picoseconds required for these populations to reach asymptotic values would be currently completely infeasible using direct dynamics. As seen, the trajectory-ensemble-averaged populations on each electronic state vary smoothly with time; however, the time dependence of individual trajectories is far more complex. For example, we observed many hops between the S_1 and T_1 states before the products $H + HCO$ were formed on T_1. Other trajectories hop multiple times between T_1 and S_0. Surface hops occur away from the exact seams of crossings between S_1 and T_1 as identified before but, as expected, in regions where two PESs come within several kilocalories per mole of each other. The distribution of energy gaps at the hopping configurations for S_1 to T_1 is shown in Figure 6a. Most of the S_1-T_1 hops occur where the energy gaps are around 6.0 kcal/mol. The hopping configurations were also examined, and most are close to the S_1 minimum geometry, where the CO internuclear distance is approximately 1.3 Å and where the energy gaps between S_1 and T_1 are close to 6 kcal/mol. Very few hops occur at the S_1/T_1 MSX, which has a more extended CO internuclear distance of about 1.6 Å. This disparity is largely a reflection of the initial Wigner phase-space distribution, which has a maximum closer to the S_1 minimum than the S_1/T_1 MSX.

The points where the surface hops between T_1 and S_0 occur most are in the formaldehyde region, as predicted by electronic structure calculations.[33] We present the distribution of energy gaps at the hopping configurations from T_1 to S_0 in Figure 6b. As seen, the distribution is very wide and extends to a large value of 70 kcal/mol, with a peak at around 40 kcal/mol. We examined the corresponding hopping geometries, and as expected, the ones with small gaps are very close to the MSX1 of S_0/T_1 (where the bending modes are excited). However, most hopping configurations are closer to the T_1 minimum, where the energy gap is large. We calculated the average hopping probability corresponding to each histogram bin shown in Figure 6b. As expected, it is largest (but only roughly 0.01) for the smallest gap and smallest (roughly 0.001) for the largest gap. That the maximum occurs roughly in the middle of this gap range is a consequence of convoluting the hopping probability with the time trajectories spend in a given "gap region".

To investigate this further, we plot the distribution of values of the most extended CH bond length (R_{CH}) at the first hop configuration from T_1 to S_0. This is shown in Figure 7, where, as seen, most of the hopping occurs with R_{CH} in the range of 1.0−1.5 Å to form either $H_2 + CO$ or $H + HCO$ products. The results for the radical products differ from the exploratory wavepacket calculations of Robb and co-workers,[35] who reported that radical products are formed from crossings with $R_{CH} > 2.0$ Å. They also reported a crossing between T_1 and S_0 with $R_{CH} > 2.0$ Å; however, the calculated MRCI/aug-cc-pVTZ SO coupling between T_1 and S_0 at that crossing is only 2.6 cm^{-1}, so hops in that part of the configuration space are expected to be negligible.

The majority of trajectories that form products on S_0 visit the S_0 global minimum before dissociating to molecular or radical products. In addition, the roaming pathway to form $H_2 + CO$ is also observed from this group of trajectories. This result supports the approach, taken in previous single-state calculations, of initiating trajectories at the global minimum of S_0.[25−28] This

dx.doi.org/10.1021/ja201559r | J. Am. Chem. Soc. 2011, 133, 7957–7968

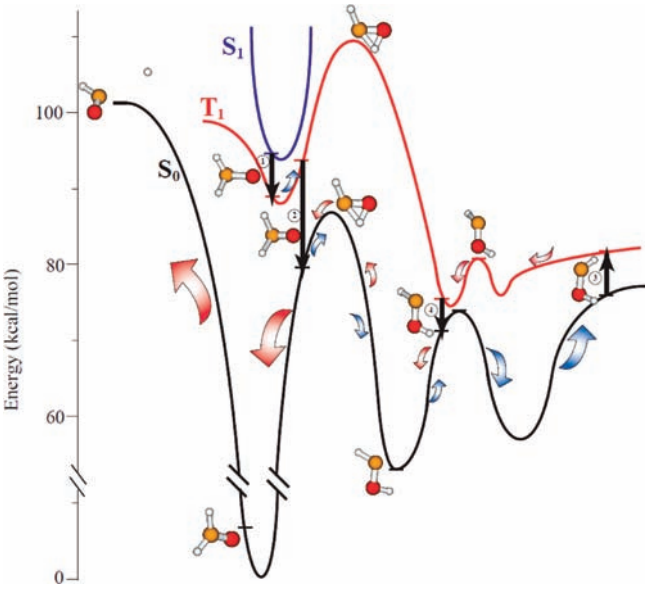

Figure 8. Schematic of the pathway for isomerization on T_1 via S_0 prior to dissociation on S_0 obtained from the present three-state trajectory surface hopping calculations. The black arrows indicate the four labeled electronic-state hops, the red curved arrows indicate the isomerization on S_0 to the hydroxycarbene region where the hop to T_1 occurs, and the blue curved arrows indicate the isomerization back to the H_2CO region followed by dissociation to H + HCO. The hop to T_1 in the hydroxycarbene region is to the isomer of H_2CO T_1 that is blocked by a large barrier relative to the T_1 minimum on T_1, reported in ref 33.

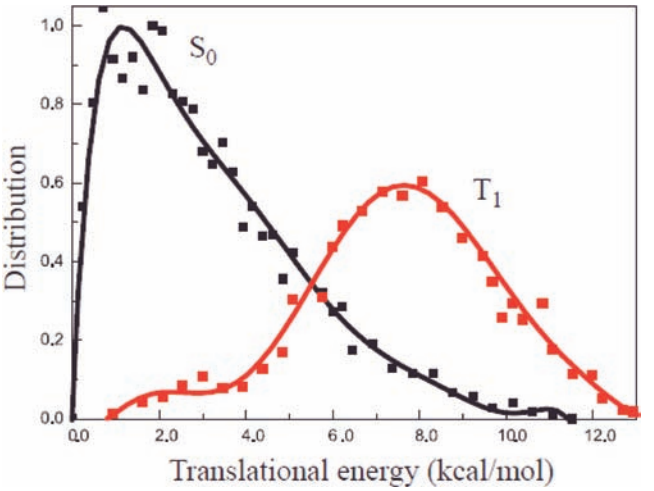

Figure 9. Translational energy distribution of H + HCO products from S_0 and T_1 at a total energy of 108.6 kcal/mol.

result is especially significant for the roaming pathway, which was discovered in these earlier calculations.

We did find an interesting new pathway that directly involves both S_0 and T_1 dynamics. It is an isomerization on T_1 that avoids the large barrier between the T_1 global minimum and the T_1 isomer by a hop from S_0. The schematic of this is shown in Figure 8. As seen, the trajectory is first initiated at the S_1 state and then hops to T_1 and then to S_0, as usual, in the region of the H_2CO structure. During the propagation on S_0, the molecule isomerizes to *trans*-HCOH and then to *cis*-HCOH and then hops back to T_1 at one *cis*-HCOH structure. After that, the molecule isomerizes to *trans*-HCOH on T_1 and then hops down to S_0 at one *trans*-HCOH structure. This particular trajectory finally dissociates to H + HCO products on S_0. Perhaps the most interesting part of this convoluted pathway is that it actually involves a net isomerization on T_1 that bypasses the high barrier mentioned above between the H_2CO structure and the T_1 HCOH structure. It does so by first hopping to S_0, where this isomerization is facile, and then "up hopping" to the analogous structure on T_1. This is, however, a minor pathway, with about 5% of the trajectories found going through this new pathway.

We consider now some general results for the radical products channel. For the first time the branching ratios of H + HCO produced from T_1 and S_0 in the photodissociation of formaldehyde are calculated in this study. Since some of the HCO products are formed with less than ZPE, the Gaussian binning (GB) method is employed to analyze the final state. The Gaussian weight is calculated according to the vibrational energy of the HCO product, and the same approach to calculate the weight for a polyatomic product was proposed by Czakó and Bowman.[63] The branching ratio of H + HCO products from S_0 and T_1 using the GB method is about 68:32 at the total energy of 108.6 kcal/mol, corresponding to a photolysis energy of 91.5 kcal/mol (312 nm). At a higher total energy of 122.1 kcal/mol, which is much higher than the barrier height of T_1, we find, as expected, that most of the radical products are generated on T_1, and the S_0 to T_1 branching ratio is 17:83. By contrast, at the lowest energy considered, 99.1 kcal/mol, nearly all the radical products are formed on the S_0 state.

As noted, the radical products H + HCO can be produced from both S_0 and T_1, while the molecular products H_2 + CO are exclusively formed on S_0. We calculated the branching ratios of the total H + HCO and H_2 + CO products. At the middle total energy of 108.6 kcal/mol, the fraction of H + HCO is about 41%, and that of H_2 + CO is 59%. This ratio becomes 76:24 at an energy of 122.1 kcal/mol, and 10:90 at an energy of 99.1 kcal/mol. The high fraction of H + HCO products at higher energy is a consequence of the fact that these products can be produced from both S_0 and T_1 and that as noted the contribution of H + HCO products from T_1 increases rapidly as the energy increases. That dissociation on T_1 to H + HCO is more likely at higher energies than surface hopping to S_0 is quite reasonable, because direct dissociation is electronically non state changing and thus more likely than dynamics that require electronic state changing.

The translational energy distributions of the H + HCO products obtained from S_0 and T_1 at the total energy of 108.6 kcal/mol are shown in Figure 9. As seen, the translational energy distribution from S_0 is broad and peaked around 1.0 kcal/mol; however, that from T_1 behaves quite differently, displaying a peak around 7.5 kcal/mol. The different behaviors support the conclusion that the dynamics on S_0 is statistical, as expected, whereas that on T_1 is dominated by the exit channel barrier. The corresponding HCO internal energy distributions reflect these differences, as reported previously by Yin et al.[14] in a joint experimental/theoretical study.

By analyzing the translational energy distributions and final rovibrational state distributions of CO and H_2, we found results similar to those obtained on the single S_0 PES by initiating the trajectories on the global minimum of the S_0 state.[25−28] The translational energy distribution at a total energy of 108.6 kcal/mol is shown in Figure 10. As seen, the distributions display a bimodal character with the major peak around 65 kcal/mol and a minor

dx.doi.org/10.1021/ja201559r |J. Am. Chem. Soc. 2011, 133, 7957–7968

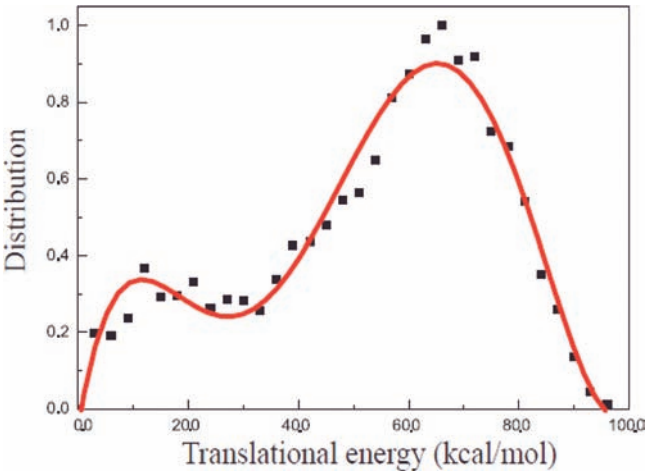

Figure 10. Translational energy distribution of H_2 + CO at a total energy of 108.6 kcal/mol.

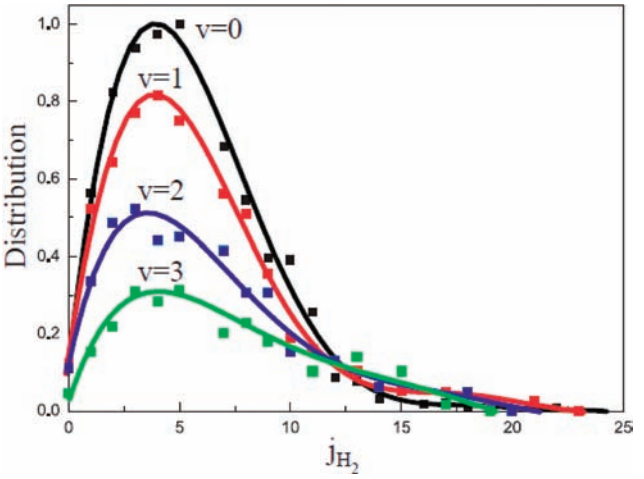

Figure 11. Final rovibrational distribution of H_2 at a total energy of 108.6 kcal/mol.

peak around 15 kcal/mol. The high translational energy peak corresponds to high j_{CO} results from the reaction via the transition state. By contrast, the low translational energy peak corresponds to the low j_{CO} shoulder in the CO rotational distribution and hot vibrational state populations of H_2, which come from the roaming pathway. As seen from the rovibrational distributions of H_2, shown in Figure 11, the H_2 products are highly vibrationally excited, but in low rotational state distributions with a peak around 4.

SUMMARY, CONCLUSIONS, AND FINAL REMARKS

In summary, we presented three-state surface hopping studies of the photodissociation dynamics of formaldehyde using global potential energy surfaces. This is the first theoretical work involving three coupled PESs, S_0, T_1, and S_1, to simulate the photodissociation of formaldehyde. The surface hopping trajectory calculations were carried out on the diabatic representation using the fewest-switches with time uncertainty algorithm. From the time dependence of the normalized populations of S_1, T_1, and S_0, we found the reaction time is on the order of several hundreds of picoseconds for the trajectories going to the products on T_1 or S_0. We found most of the hops occur at configurations away from the exact minimum energy crossings between S_1 and T_1 or T_1 and S_0 and are closer to the S_1 minimum for S_1/T_1 hops and the T_1 minimum for T_1/S_0 hops. We reported a new isomerization pathway on T_1 to the HCOH region, in which a hop occurs from T_1 to S_0 in the formaldehyde region, followed by isomerization on S_0 to *trans*-HCOH or *cis*-HCOH, and then a hop to the T_1 state in the HCOH region. After some time on T_1, the trajectory hops down to S_0 and subsequently dissociates.

The branching ratios of radical products produced from S_0 and T_1 states and those of total radical products and molecular products were calculated and discussed at three different total energies. The branching ratios depend sensitively on the total energy relative to the radical product barrier height of the T_1 PES. Finally, the translational energy distributions of the H + HCO and CO and H_2 products were calculated. The former translational energy distribution obtained from the S_0 state is statistical, and that from the T_1 state displays an impulsive character with a higher peak around 7.5 kcal/mol. The translational energy distributions and final rovibrational distributions of CO and H_2 products were found to be similar to the previous dynamics calculations initiated and integrated on S_0 alone. The hot rotational state of CO and cold vibrational state of H_2 result from the reaction via the well-known transition state, while the low CO rotational distribution of CO and high vibrational population of H_2 come from the "roaming" pathway.

We end this section with some general remarks about the approximations inherent in the surface hopping calculations. First, we note that there are many so-called "frustrated hops", that is, transitions that would violate conservation of energy. The "time uncertainty" extension of Truhlar and co-workers permits these to occur using an approximate algorithm. This extension is important because such transitions can occur quantum mechanically. Another quantum effect that is absent in trajectory calculations is zero-point energy. Classically, reaction products with less than zero-point vibrational energy can be formed. For the present case this is a very minor issue for the molecular products H_2 + CO, but as expected, it is a major issue for the radical products H + HCO, especially at and just above the threshold energy for these products. This has already been noted in previous single-surface calculations.[27,28]

Beyond these general approximations in surface hopping calculations, the use of a constant spin−orbit coupling (except asymptotically) and the neglect of any coupling between S_1 and S_0 are additional approximations. Thus, even though the present calculations are at the current state-of-the-art, we acknowledge that quantum approaches to electronically nonadiabatic reactions are clearly desirable.

ASSOCIATED CONTENT

Supporting Information. Complete refs 38, 44, and 49. This material is available free of charge via the Internet at http://pubs.acs.org.

AUTHOR INFORMATION

Corresponding Author
jmbowma@emory.edu

Present Addresses
[†]Georgia Gwinnett College, Lawrenceville, GA 30043, United States.

■ ACKNOWLEDGMENT

We thank the Department of Energy (Grant DE-FG02-97ER14782) for financial support.

■ REFERENCES

(1) Moore, C. B.; Weisshaar, J. C. *Annu. Rev. Phys. Chem.* **1983**, *34*, 525.
(2) Bamford, D. J.; Filseth, S. V.; Foltz, M. F.; Hepburn, J. W.; Moore, C. B. *J. Chem. Phys.* **1985**, *82*, 3032.
(3) Butenhoff, T. J.; Carleton, K. L.; Moore, C. B. *J. Chem. Phys.* **1990**, *92*, 377.
(4) Green, W. H.; Moore, C. B.; Polik, W. F. *Annu. Rev. Phys. Chem.* **1993**, *43*, 591.
(5) van Zee, R. D.; Foltz, M. F.; Moore, C. B. *J. Chem. Phys.* **1993**, *99*, 1664.
(6) Suits, A. *Acc. Chem. Res.* **2008**, *41*, 873.
(7) Herath, N.; Suits, A. G. *J. Phys. Chem. Lett.* **2011**, *2*, 642.
(8) Chuang, M. C.; Foltz, M. F.; Moore, C. B. *J. Chem. Phys.* **1987**, *87*, 3855.
(9) Terentis, A. C.; Kable, S. H. *Chem. Phys. Lett.* **1996**, *258*, 626.
(10) Dulligan, M. J.; Tuchler, M. F.; Zhang, J.; Kolessov, A.; Wittig, C. *Chem. Phys. Lett.* **1997**, *276*, 84.
(11) Valachovic, L. R.; Tuchler, M. F.; Dulligan, M. J.; Droz-Georget, Th.; Zyrianov, M.; Kolessov, A.; Reiser, H.; Wittig, C. *J. Chem. Phys.* **2000**, *112*, 2752.
(12) Terentis, A. C.; Waugh, S. E.; Metha, G. F.; Kable, S. H. *J. Chem. Phys.* **1998**, *108*, 3187.
(13) Yin, H.-M.; Nauta, K.; Kable, S. H. *J. Chem. Phys.* **2005**, *122*, 194312.
(14) Yin, H.-M.; Kable, S. H.; Zhang, X.; Bowman, J. M. *Science* **2006**, *311*, 1443.
(15) Hopkins, W. S.; Loock, H. P.; Cronin, B.; Nix, M. G. D.; Devine, A. L.; Dixon, R. N.; Ashfold, M. N. R. *J. Chem. Phys.* **2007**, *127*, 064301.
(16) Carbajo, P. G.; Smith, S. C.; Holloway, A. L.; Smith, C. A.; Pope, F. D.; Shallcross, D. E.; Orr-Ewing, A. J. *J. Phys. Chem A* **2008**, *112*, 12437.
(17) Hopkins, W. S.; Loock, H. P.; Cronin, B.; Nix, M. G. D.; Devine, A. L.; Dixon, R. N.; Ashfold, M. N. R.; Yin, H. M.; Rowling, S. J.; Bull, A.; Kable, S. H. *J. Phys. Chem. A* **2008**, *112*, 9283.
(18) Feller, D.; Dupuis, M.; Garrett, B. C. *J. Chem. Phys.* **2000**, *113*, 218.
(19) Chang, Y.-T.; Minichino, C.; Miller, W. H. *J. Chem. Phys.* **1992**, *96*, 4341.
(20) Chang, Y.-T.; Miller, W. H. *J. Phys. Chem.* **1990**, *94*, 5884.
(21) Chen., W.; Hase, W. L.; Schlegel, H. B. *Chem. Phys. Lett.* **1994**, *228*, 436.
(22) Peslherbe, G. H.; Hase, W. L. *J. Chem. Phys.* **1996**, *104*, 7882.
(23) Li, X.; Millam, J. M.; Schlegel, H. B. *J. Chem. Phys.* **2000**, *113*, 10062.
(24) Townsend, D.; Lahankar, S. A.; Lee, S. K.; Chambreau, S. D.; Suits, A. G.; Zhang, X.; Rheinecker, J.; Harding, L. B.; Bowman, J. M. *Science* **2004**, *306*, 1158.
(25) Zhang, X.; Rheinecker, J. L.; Bowman, J. M. *J. Chem. Phys.* **2005**, *122*, 114313.
(26) Lahankar, S. A.; Chambreau, S. D.; Townsend, D.; Suits, F.; Farnum, J.; Zhang, X.; Bowman, J. M.; Suits, A. G. *J. Chem. Phys.* **2006**, *125*, 044303.
(27) Bowman, J. M.; Zhang, X. *Phys. Chem. Chem. Phys.* **2006**, *8*, 321.
(28) Bowman, J. M.; Shepler, B. C. *Annu. Rev. Phys. Chem.* **2011**, *62*, 53.
(29) Zhang, X.; Zhou, S.; Harding, L. B.; Bowman, J. M. *J. Phys. Chem. A* **2004**, *108*, 8980.
(30) Simonsen, J. B.; Rusteika, N.; Johnson, M. S.; Sølling, T. I. *Phys. Chem. Chem. Phys.* **2008**, *10*, 674.
(31) Araujo, M.; Lasorne, B.; Bearpark, M. J.; Robb, M. A. *J. Phys. Chem. A* **2008**, *112*, 7489.
(32) Shepler, B. C.; Epifanovsky, E.; Zhang, P.; Bowman, J. M.; Krylov, A. I.; Morokuma, K. *J. Phys. Chem. A* **2008**, *112*, 13267.
(33) Zhang, P.; Maeda, S.; Morokuma, K.; Braams, B. J. *J. Chem. Phys.* **2009**, *130*, 144304.
(34) Maeda, S.; Ohno, K.; Morokuma, K. *J. Phys. Chem. A* **2009**, *113*, 1704.
(35) Araujo, M.; Lasorne, B.; Bearpark, M. J.; Magalhaes, A. L.; Worth, G. A.; Bearpark, M. J.; Robb, M. A. *J. Chem. Phys.* **2009**, *131*, 144301.
(36) Araujo, M.; Lasorne, B.; Magalhaes, A. L.; Bearpark, M. J.; Robb, M. A. *J. Phys. Chem. A* **2010**, *114*, 12016.
(37) Worth, G. A.; Beck, M. H.; Jackle, A.; Burghardt, I.; Lasome, B.; Mayer, H. D. *The MCTDH Package*, development version 9.0; University of Heidelberg: Heidelberg, Germany, 2008.
(38) Frisch, M. J.; Trucks, G. W.; Schlegel, H. B; *Gaussian Development Version*, revision G.01; Gaussian, Inc.: Wallingford, CT, 2007.
(39) Tully, J. C.; Preston, R. K. *J. Chem. Phys.* **1971**, *55*, 562.
(40) Tully, J. C. *J. Chem. Phys.* **1990**, *93*, 1061.
(41) Jasper, A. W.; Truhlar, D. G. *Chem. Phys. Lett.* **2003**, *369*, 60.
(42) This was actually done for the simpler problem (from the electronic structure aspect) of electronic quenching of OH ($A\,^2\Sigma^+$) by H_2. We carried out direct-dynamics calculations of this quenching with the Newton-X program package,[43] which uses Tully's algorithm with the Columbus quantum chemistry program,[44] to calculate the energies, forces, and nonadiabatic derivative coupling. We used the same CASSCF level of ab initio theory and smaller basis (cc-pVDZ) used by Robb and co-workers for H_2CO. We found it took a lot of CPU time to do this kind of direct dynamics calculation, about 7 h for the quite small 6-31g basis, 8 h for the cc-pVDZ basis, and 32 h for the cc-pVTZ basis on a single core. Therefore, a total of several hundred trajectories were run using the CASSCF/cc-pVDZ level, and electronic transitions occurred only on 3% of the total trajectories. We randomly selected some trajectories without surface hopping and compared the CASSCF energies along those trajectories to the CASSCF energies calculated by the MRCI(Q)/aug-cc-pVTZ level, and we found that the energy differences between them were a little large, with a maximum difference of 30% especially near the conical intersections of the excited and ground states. The reason why most of the trajectories stayed on the excited state without surface hopping was that the CASSCF level of ab initio theory could not describe the system well. Also it is impossible for other high levels such as MRCI calculations to be used in the direct dynamics because of time costs. Thus, based on these results, we abandoned the direct-dynamics approach for the present three-state dynamics calculations of H_2CO photodissociation.
(43) Baratti, M.; Granucci, G.; Ruckenbauer, M.; Pittner, J.; Persico, M.; Lischka, H. Newton-X, a package for Newtonian dynamics close to the crossing seam, version 1.2.
(44) Lischka, H.; Shepard, R.; Columbus, an ab initio electronic structure program, release 5.9.1, 2006.
(45) Li, Z. H.; Jasper, A. W.; Bonhommeau, D. A.; Valero, R.; Truhlar, D. G. *ANT2009*; University of Minnesota: Minneapolis, MN, 2009.
(46) Farnum, J. D.; Zhang, X.; Bowman, J. M. *J. Chem. Phys.* **2007**, *126*, 134305.
(47) Troe, J.; Ushakov, V. *J. Phys. Chem. A* **2007**, *111*, 6610.
(48) Braams, B. J.; Bowman, J. M. *Int. Rev. Phys. Chem.* **2009**, *28*, 577.
(49) Werner, H.-J.; Knowles, P. J.; Amos, R. D.; MOLPRO, version 2008.1, a package of ab initio programs.
(50) Koga, N.; Morukuma, K. *Chem. Phys. Lett.* **1985**, *119*, 371.
(51) Hu, W.; Lendvay, G.; Maiti, B.; Schatz, G. C. *J. Phys. Chem. A* **2008**, *112*, 2093.
(52) Pattengill, M. D. *Chem. Phys.* **1983**, *75*, 59.
(53) Schinke, R. *J. Phys. Chem.* **1988**, *92*, 3195.
(54) Untch, A.; Henning, S.; Schinke, R. *Chem. Phys.* **1988**, *126*, 181.
(55) Corderio, M. N. D. S.; Martínez-Núñez, E.; Fernández-—Ramos, A.; Vázquez, S. A. *Chem. Phys. Lett.* **2003**, *381*, 37.
(56) Schinke., R. *Photodissociation Dynamics*; Cambridge University Press: Cambridge, U.K., 1993.

(57) Christoffel, K. M.; Bowman, J. M. *J. Chem. Phys.* **1996**, *104*, 8348.
(58) Rubinstein, R. Y. *Simulation and the Monte Carlo Method*; John Wiley and Sons, Inc.: New York, 1981.
(59) Guo., H.; Murrell, J. N. *Mol. Phys.* **1988**, *65*, 821.
(60) Engel, V.; Schinke, R. *J. Chem. Phys.* **1988**, *88*, 6831.
(61) Miller, R. G.; Lee, E. K. C. *J. Chem. Phys.* **1978**, *68*, 4448.
(62) Weisshaar, J. C.; Moore, C. B. *J. Chem. Phys.* **1980**, *72*, 5415.
(63) Czakó, G.; Bowman, J. M. *J. Chem. Phys.* **2009**, *131*, 244302.